

A PID-Based Speed Modulation Method for Left Ventricular Assist Devices

Ziteng Tong¹, Zhe Gou², Jianping Tan^{2*}

¹The Light Alloy Research Institute, Central South University, Changsha, China

²The College of Mechanical and Electrical Engineering, Central South University, Changsha, China

Email: 1649947391@qq.com, gouzhe@csu.edu.cn, *jptan@csu.edu.cn

How to cite this paper: Tong, Z.T., Gou, Z. and Tan, J.P. (2025) A PID-Based Speed Modulation Method for Left Ventricular Assist Devices. *Open Journal of Applied Sciences*, 15, 3780-3794.

<https://doi.org/10.4236/ojapps.2025.1511245>

Received: November 11, 2025

Accepted: November 23, 2025

Published: November 26, 2025

Copyright © 2025 by author(s) and Scientific Research Publishing Inc.

This work is licensed under the Creative Commons Attribution International License (CC BY 4.0).

<http://creativecommons.org/licenses/by/4.0/>



Open Access

Abstract

Although left ventricular assist devices (LVADs) have been widely used for patients with end-stage heart failure (HF), their speed modulation remains a challenge. Currently, the speed is set by physicians, predominantly relying on their empirical judgment, and remains fixed during long-term support. The optimal speed varies significantly among patients due to individual differences in physiological status, the severity of heart failure, and the specific LVAD product implanted. In this work, we proposed a PID-based controller to obtain the optimal speed which satisfies the demands of different patients. Physiological indicators such as the mean aortic flow rate and the mean aortic pressure are chosen as control targets. After each cardiac cycle, these indicators are transferred to the PID controller in order to adjust the pump speed. This PID-based controller is then validated numerically on a cardiovascular system-LVAD coupling model. Results show that the proposed controller is able to find the optimal speed in both the flow rate control mode and the pressure control mode. The PID-base controller is further tested for two different LVADs. The same cardiac outputs are obtained, proving its robustness and universality. This method offers a simple, robust, and model-free framework for adapting LVAD support to the needs of HF patients. It can help physicians to determine the initial pump speed, and also enable autonomous speed modulation for HF patients with long-term LVAD support.

Keywords

Left Ventricular Assist Device, Physiological Control System, PID Control

1. Introduction

Heart failure (HF) remains a global public health issue with escalating prevalence and morbidity, posing a significant burden on healthcare systems worldwide [1].

For patients with end-stage HF, heart transplantation is the gold standard therapeutic option. However, the shortage of suitable donor hearts severely limits its application [2]. In this context, mechanical circulatory support, particularly the rotary blood pump (RBP) type left ventricular assist device (LVAD), has emerged as a standard of care, serving not only as a bridge to transplantation but also as a destination therapy for ineligible candidates [3].

The primary function of an LVAD is to unload the left ventricle and maintain adequate peripheral perfusion. Clinically, the operating speed of an LVAD is a critical parameter that determines the level of cardiac support. The optimal speed varies significantly among patients due to individual differences in physiological status, the severity of heart failure, and the specific LVAD product implanted [4]. An inappropriately set speed can lead to severe complications. For instance, insufficient speed fails to provide adequate ventricular unloading, while excessive speed may cause ventricular suction, inadequate aortic valve opening, or even gastrointestinal bleeding [5]. Currently, in clinical practice, the initial speed setting predominantly relies on the empirical judgment of physicians, guided by hemodynamic monitoring and echocardiographic evaluation. Once set, this speed typically remains fixed during long-term support. Moreover, a fixed, physician-set LVAD speed is inherently non-physiological. It cannot accommodate the patient's long-term progression (e.g., myocardial recovery or further deterioration) or short-term variations in activity (e.g., rest vs. exercise).

The limitations of fixed-speed operation have motivated extensive research into physiological control systems that can automatically adjust LVAD speed in response to the patient's changing demands. Some strategies aim to maintain a constant pressure difference across the pump, which is theorized to mimic the native Frank-Starling mechanism [6]. Another prominent approach utilizes the inherent pulsatility of the pump flow as control objective, which reflects the residual contractility of the native heart. Algorithms that maximize or maintain a target pulsatility index have been developed and tested in simulations and mock loops [7]. Other studies have explored using direct or indirect physiological signals as feedback, such as maintaining a target mean aortic pressure or estimating left atrial pressure [8]. Despite these advancements, many proposed algorithms are complex, require precise patient-specific cardiovascular models, or rely on signals that are difficult to measure continuously in an ambulatory patient [9]. There is a clear need for a robust, simple, and reliable control strategy that can be effectively implemented with available or easily estimated signals.

To address this critical gap, this paper proposes a simple automatic speed modulation method based on a proportional-integral-derivative (PID) controller. It utilizes the mean aortic flow as the primary control target, which is a direct indicator of the total cardiac output and is easy to be measured clinically. The PID controller automatically adjusts the LVAD speed to maintain the mean aortic flow at a predefined physiological setpoint, thereby ensuring adequate perfusion while promoting ventricular unloading. This method offers a simple, robust, and

model-free framework for adapting LVAD support to the dynamic needs of the patient. The subsequent sections of this paper will detail the development, simulation, and evaluation of this proposed PID-based control system.

2. Methods

2.1. Cardiovascular System-LVAD Coupling Model

A lumped-parameter model of cardiovascular system coupled with LVAD is constructed to test the performance of the proposed PID control algorithm. The cardiovascular system model consists of left heart, right heart, systemic circulation, and pulmonary circulation, as shown in **Figure 1** [10]. In each section, hemodynamic factors such as resistance, compliance and valve are represented by resistor, capacitor and diode. The relationship between these hemodynamic factors is characterized by the Kirchhoff's law. In this work, a cardiovascular system model mimics a HF patient is considered, and all the parameter values used in this model are presented in **Table 1**.

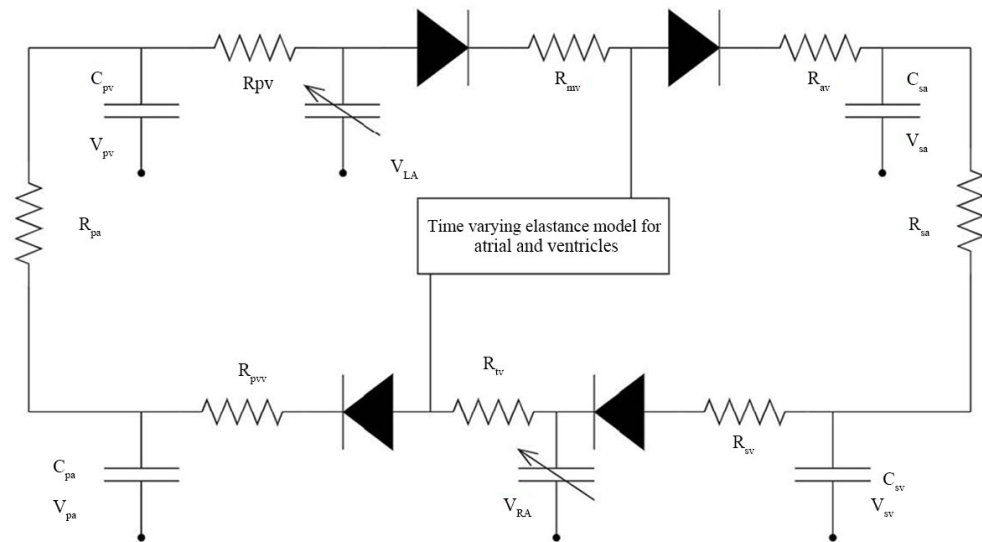


Figure 1. Schematic of the cardiovascular system model.

Table 1. Cardiovascular system parameters.

	Parameter	Value	Corresponding physiological significance
Resistance (mmHg*s/ml)	Rav	300	Aortic valve resistance
	Rsv	3333	Vena Cava resistance
	Rsa	100,000	Peripheral resistance
	Rtv	600	Tricuspid valve resistance
	Rpvv	1500	Pulmonary valve resistance
	Rpa	13,000	Pulmonary Artery resistance
	Rpv	2000	Pulmonary vein resistance
	Rmv	4000	Mitral valve resistance

Continued

Capacitance (ml/mmHg)	Csa	0.013	Aortic Compliance
	Csv	0.525	Venous Compliance
	Cpa	0.01	Pulmonary artery compliance
	Cpv	0.12	Pulmonary vein compliance
Volume (ml)	Vsa	650	Body arterial volume
	Vsv	3800	Body vein volume
	Vra	12.5	Right atrial volume
	Vpa	250	Pulmonary Artery volume
	Vpv	550	Pulmonary vein volume
	Vla	12.5	Left atrial volume

The LVAD bridges the left ventricle and the aorta, as shown in **Figure 1**. A parameter-based pump model is used to describe the hydrodynamic characteristics of the RBP:

$$H_{LVAD} = a_0\omega^2 + a_2\omega Q_{LVAD} + a_3\omega + a_4Q_{LVAD}^2$$

where ω is the pump speed in rpm, Q_{LVAD} is the pump flow rate, and H_{LVAD} is the pump pressure difference, respectively. a_0 , a_1 , a_2 and a_3 are constants fitted by experimental results of two commercial LVADs HeartMate 3 and Corheart 6 [11] [12], and their values are shown in **Table 2**.

Table 2. Constants of LVAD model.

LVAD	Parameter	Value	Unit
HeartMate 3	a_0	3.49	rpm ²
	a_1	0.73783	rpm·ml/s
	a_2	0	rpm
	a_3	-2.2706	ml ² /s ²
Corheart 6	a_0	8.438	rpm ²
	a_1	1.017	rpm·ml/s
	a_2	0.4254	rpm
	a_3	-1.3052	ml ² /s ²

2.2. PID Controller Design

The PID control system is shown in **Figure 2**. In order to maintain adequate cardiac output for HF patients, the mean aortic flow rate \bar{Q}_{ao} and the mean aortic pressure \bar{P}_{ao} are chosen as control objects. These values are obtained after each cardiac cycle, and then transferred to the PID controller. After comparing with pre-settled values, the desired pump speed is calculated by following equation:

$$\omega(\tau) = K_p(V - V_0) + K_i \int_0^\tau (V - V_0) d\tau + K_d \frac{d}{d\tau}(V - V_0)$$

where V and V_0 indicate the control object and the pre-settled value, and K_p , K_i , and K_d are control parameters. The PID gain values (K_p , K_i , K_d) were selected through an empirical tuning process. This tuning process was based on simulation tests, where the controller gains were adjusted through trial and error to achieve the desired dynamic response. The goal was to ensure system stability and rapid convergence under various operating conditions, which is crucial for effective control of the LVAD pump speed. It should be noted that the equation above is not defined over time t , but over heartbeat τ , where T is the total heartbeat. In each cardiac cycle, the pump speed remains unchanged, and its value is updated once per heartbeat. Hence the integral and the differential terms are calculated in a discrete manner. Once the pump speed is updated, the cardiac output in the next cycle can be simulated by the cardiovascular system model.

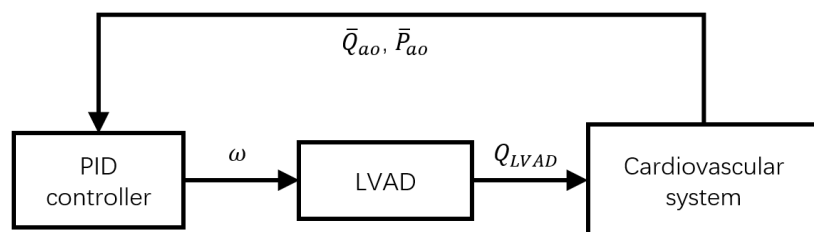


Figure 2. Schematic of the PID control system. \bar{Q}_{ao} and \bar{P}_{ao} are the mean aortic flow rate and pressure, Q_{LVAD} is the pump flow rate, and ω is the pump speed in rpm.

2.3. Simulation Procedures and Data Analysis

The efficiency and robustness of the proposed PID controller is evaluated numerically for a HF patient represented by the cardiovascular system-LVAD coupling model. The simulated heart rate is 75 beat per minute, corresponding to a cardiac cycle of 800 ms. The initial pump speed is set as 0 rpm. Then it is adjusted by the PID controller until a pre-defined mean aortic flow rate or mean aortic pressure is reached, satisfying the demand of a healthy human. It should be noted that the mean aortic flow and pressure are assumed to be directly measured in this simulation study. This assumption simplifies the modeling process; however, in real clinical applications, measuring total aortic inflow is challenging and would likely require additional sensors or a virtual-sensing strategy based on pressure and electrical variables. The aortic flow rate and the aortic pressure are assumed to be directly measured for PID control. The parameters of the PID controller remain unchanged for all tests reported in this work. All simulations are stopped once the pump speed reach a steady state. Physiological parameters such as LV volume, LV pressure, aortic flow rate, aortic pressure, etc. are obtained for data analysis.

3. Results

3.1. Mean Aortic Flow Rate Control

All flow-target experiments follow the same protocol: heart rate 75 bpm (≈ 800 ms per cycle), initial speed = 0 rpm, aortic flow/pressure assumed directly measura-

ble, and unchanged PID gains across all tests. The controller raises speed automatically until the mean aortic flow reaches the predefined setpoint; simulations stop when speed settles. **Figures 3-5** summarize PV loops, steady waveforms, and beat-averaged trends.

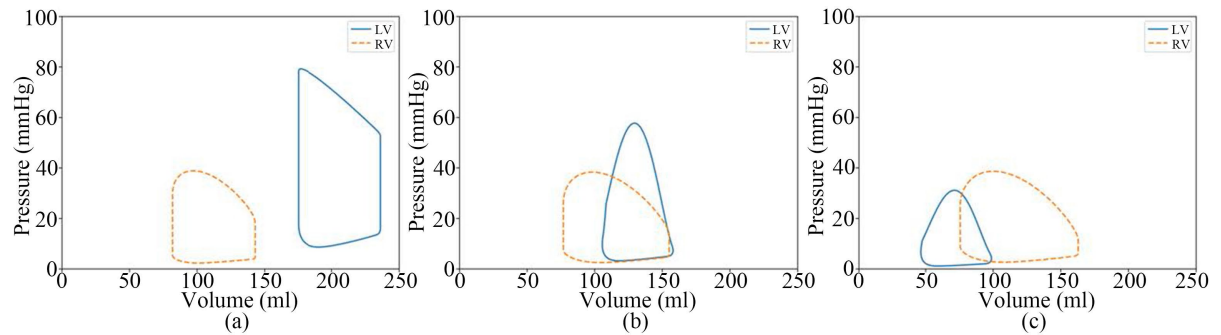


Figure 3. PV loops at pre-assist, 5.4 L/min, and 6.0 L/min.

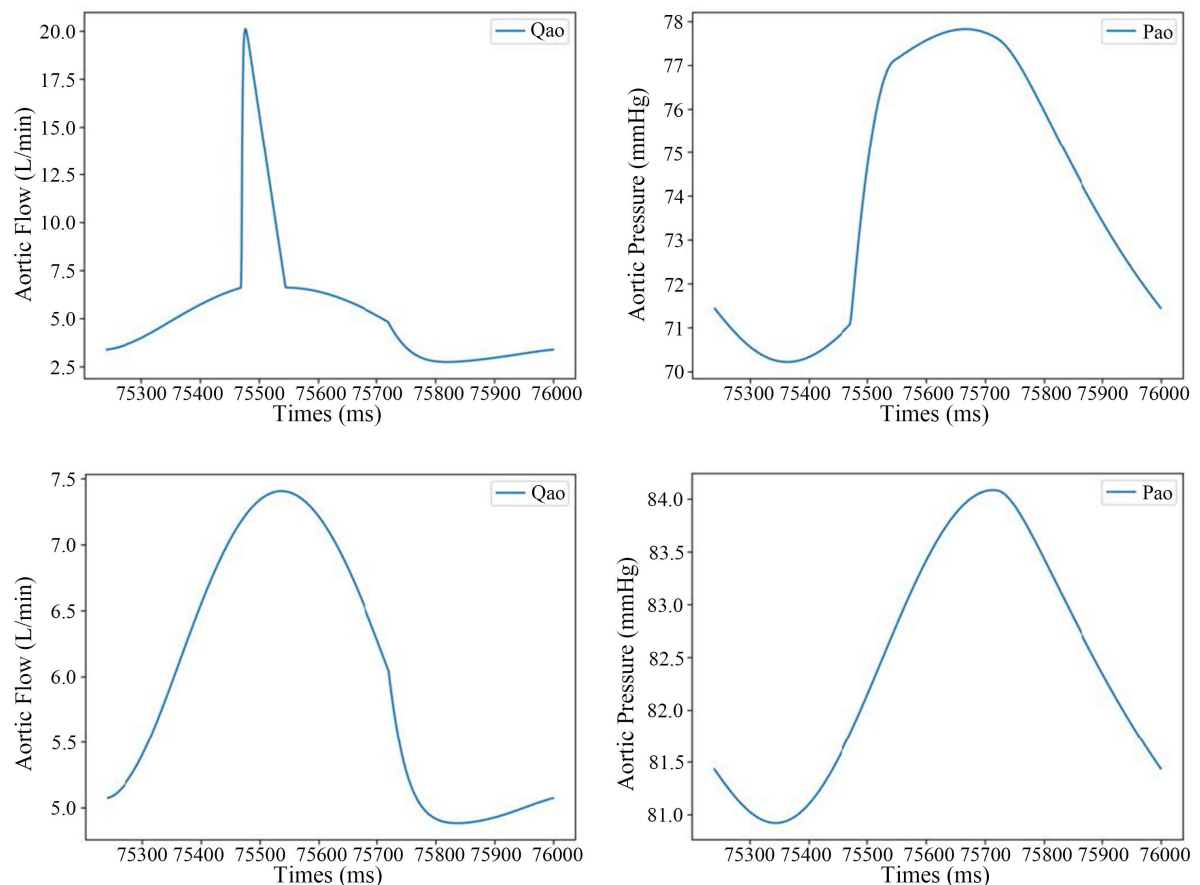


Figure 4. Aortic flow and pressure at steady state for both setpoints. Top: 5.4 L/min; bottom: 6 L/min.

At the 6.0 L/min setpoint, the beat-averaged flow exhibits a single under-damped peak $\approx 7.5 - 8.0$ L/min within the first 10 - 20 beats, then decays exponentially to target; the steady-state speed ≈ 5.68 kRPM. At 5.4 L/min, the peak is smaller, settling is faster, and steady-state speed ≈ 4.68 kRPM. The speed trajectory follows the

mean-flow envelope in phase—consistent with a beat-scale “second-order + integral” behavior shaped by peripheral resistance/compliance plus the integrator.

With the other pump, the same flow setpoints are reached at ≈ 2.80 and ≈ 3.18 kRPM, implying a higher effective static gain of its pump map around these operating points. Despite static-gain differences, damping and settling (in beats) remain comparable under identical PID gains.

We use mean-value filtering and take the derivative on the mean, which suppresses intrabeat ripples so the controller reacts to the beat-to-beat envelope; speed limits 2 - 9 kRPM with back-calculation anti-windup prevent integrator accumulation during saturation. Baseline gains: $K_p = 30$ (kRPM)/(L/s), $K_i = 8$ s^{-1} , $K_d = 0.3$ kRPM $\cdot s^{-1}\cdot L^{-1}$.

As targets increase, the pump’s share rises and the aortic-valve opening fraction drops. On PV loops this appears as a left-downward shift with a slimmer loop area—evidence of stronger LV unloading. Lower flow targets place the operating point farther from frequent valve-opening regimes, attenuating nonlinearities and reducing transient peaks; conversely, higher targets achieve faster approach but require higher steady-state speeds. Under tested gains, no suction was observed, consistent with the chosen limits and mean-filtering.

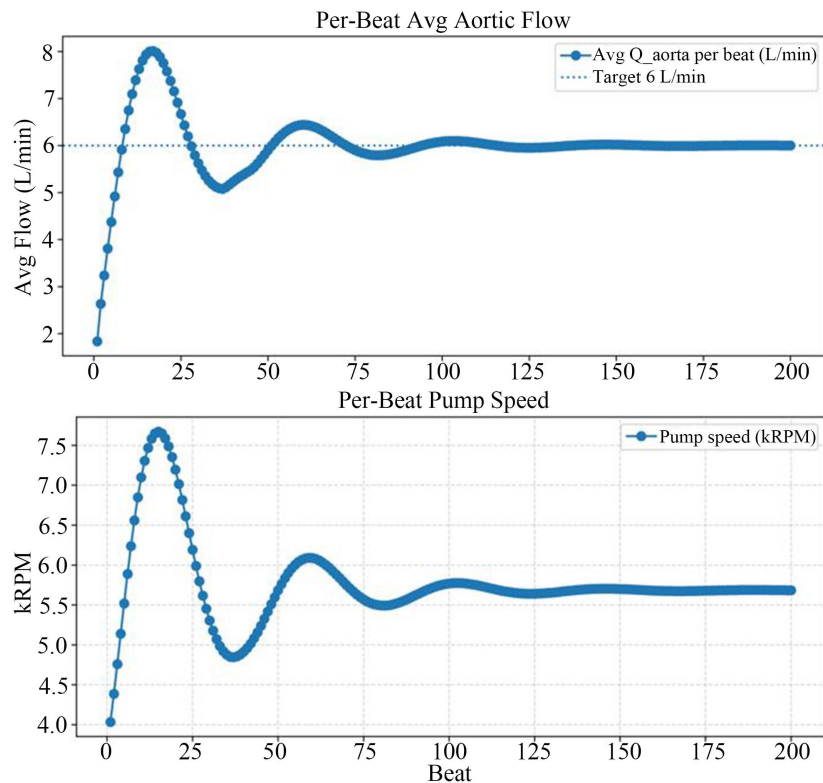


Figure 5. Beat-averaged aortic flow and pump speed vs. beat index.

3.2. Mean Aortic Pressure Control

When MAP = 85/95 mmHg is targeted, beat-to-beat responses remain lightly underdamped with exponential convergence. One device settles at $\approx 3.28/3.73$ kRPM; for

HeartMate 3 the corresponding speeds are $\approx 5.88/6.68$ kRPM, illustrating the monotonic mapping “higher MAP \rightarrow higher speed” and device-specific pump-map gains. **Figures 6-8** summarize PV loops, steady waveforms, and beat-averaged trends.

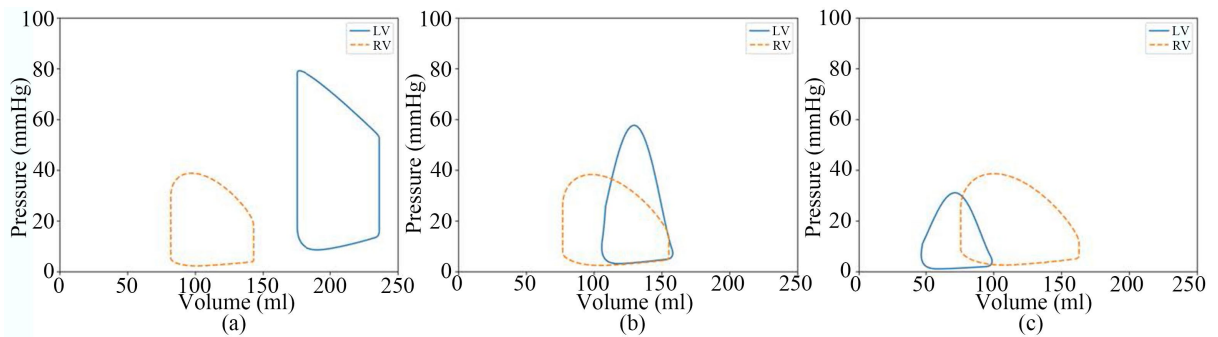


Figure 6. PV loops at pre-assist, MAP = 85 and 95 mmHg.

Steady waveforms and beat-averaged MAP/speed trajectories indicate similar damping to flow-target control yet greater sensitivity to peripheral resistance; overshoot and settling remain acceptable with the tested gains.

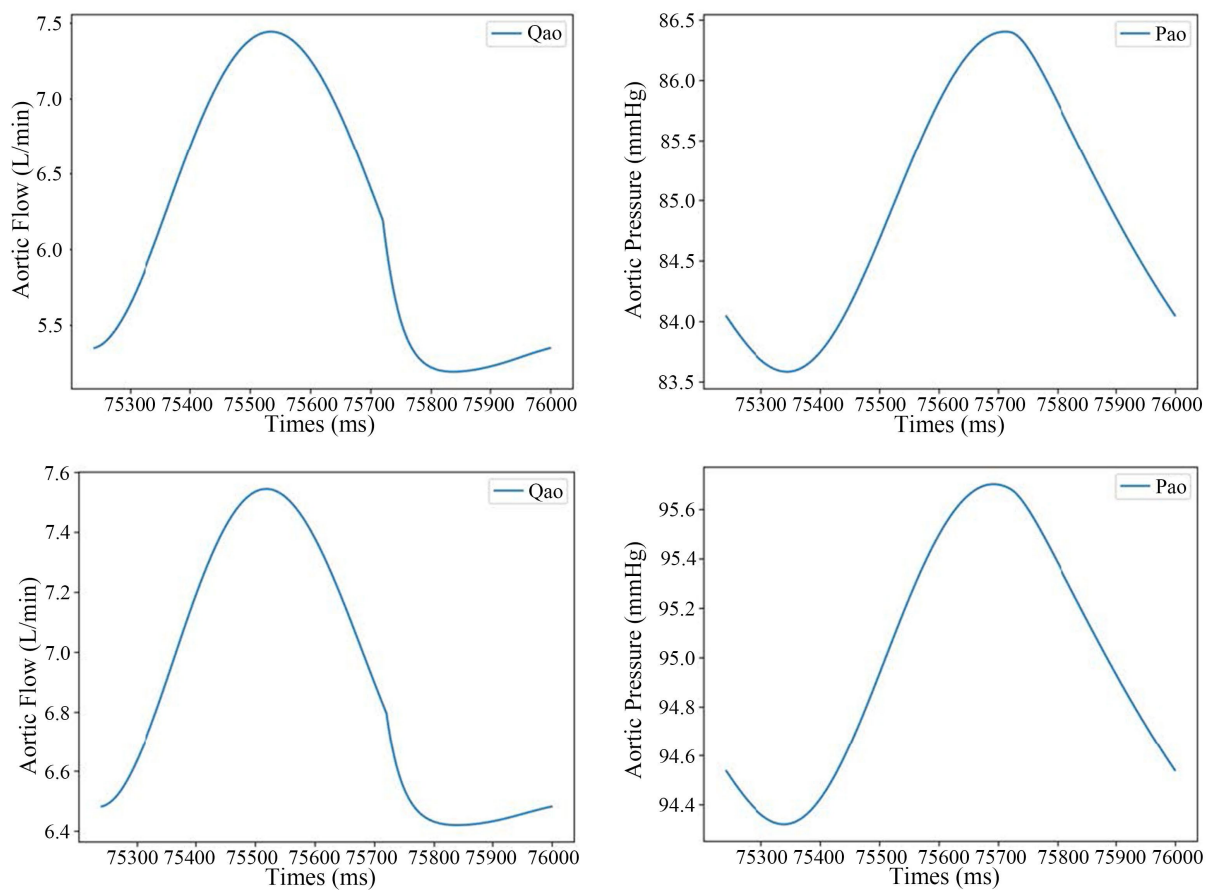


Figure 7. Aortic flow and pressure at steady state for both MAP targets. Top: 85 mmHg; bottom: 95 mmHg.

All pressure-target experiments share the same PID gains, mean-value filtering,

derivative on mean, and speed limits—ensuring fair side-by-side comparison across devices/targets. At MAP targets, increased afterload demands higher steady-state speed; PV loops still demonstrate unloading while preserving physiologic valve timing under the tested range—consistent with safe operation within the 2 - 9 kRPM limits.

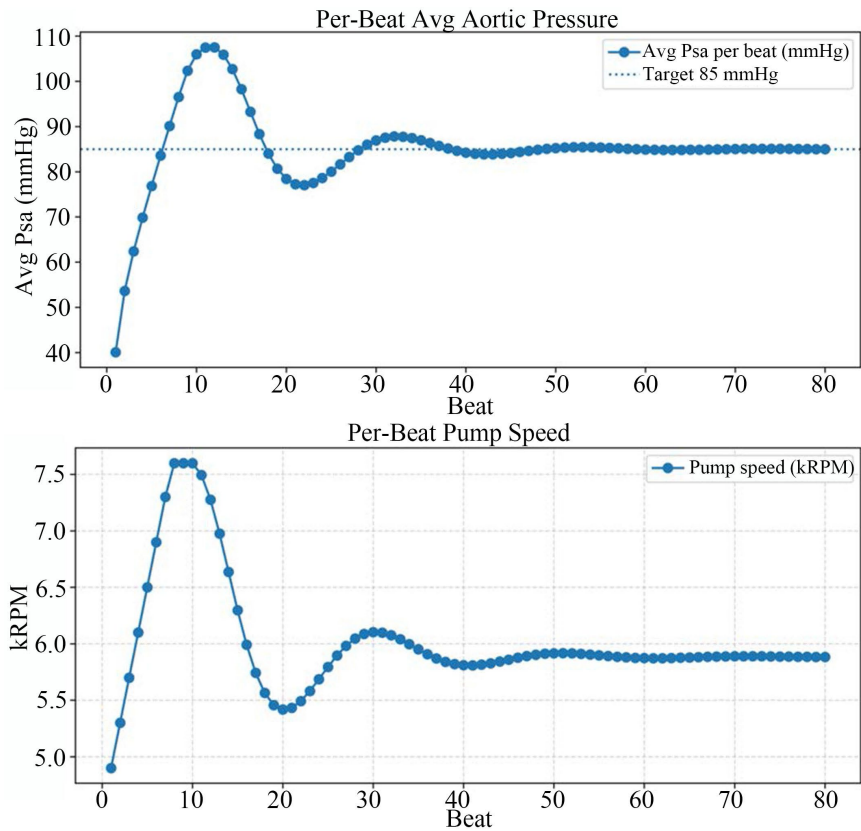


Figure 8. Beat-averaged MAP and pump speed vs. beat index.

3.3. Comparison of Different LVADs

To ensure a fair device-to-device comparison, both HeartMate 3 and Corheart 6 were tested under the same controller and protocol: HR = 75 bpm, initial speed = 0 rpm, identical PID gains, and the same measurement chain (mean-value filtering with derivative on mean, plus speed limits 2 - 9 kRPM with back-calculation anti-windup). All trials ended after the speed converged to steady state. This alignment means any cross-device differences mainly reflect the pump maps rather than tuning or protocol artifacts.

Under mean-flow targets, HeartMate 3 reaches 6.0 L/min with a steady-state speed of about 5.68 kRPM and 5.4 L/min at about 4.68 kRPM, with a lightly under-damped transient (single peak \approx 7.5 - 8.0 L/min within the first 10 - 20 beats). Corheart 6 attains the same two flow setpoints at \approx 2.80 kRPM and \approx 3.18 kRPM (at the two setpoints), indicating a higher effective static gain around these operating points. Despite this static-gain difference, the damping and settling (in beats) are broadly similar between devices when gains are kept identical.

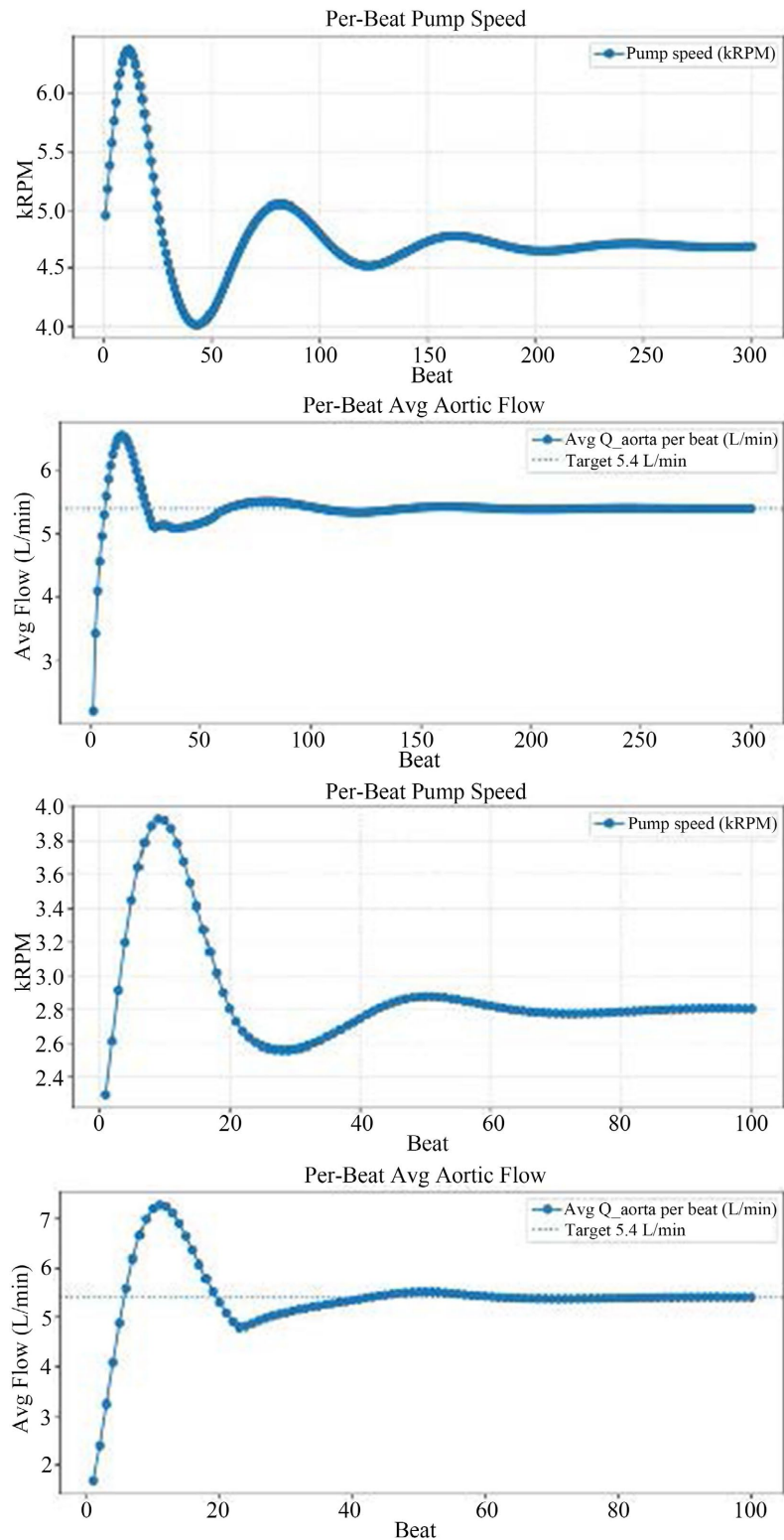


Figure 9. Per-beat pump speed and average aortic flow under the same closed-loop controller (target = 5.4 L/min). Top: HeartMate 3; bottom: Coheart 6. Both pumps show lightly under-damped transients and converge to the reference.

When targeting MAP = 85/95 mmHg, Corheart 6 settles at approximately

3.28/3.73 kRPM, while HeartMate 3 requires approximately 5.88/6.68 kRPM to achieve the same pressures. These results reaffirm the monotonic mapping “higher MAP → higher steady-state speed,” and again emphasize that the principal cross-device difference is the speed required by the respective pump maps, not the transient shape itself, which remains lightly under-damped with exponential convergence (Beat-averaged MAP/speed trajectories are summarized in **Figure 9**).

Across both targets, the transient envelopes of the two devices look alike at the same gains—rise, single modest overshoot, and settling within several beats—while the steady operating point differs due to pump-map gain. Physiologically, as either the target or the effective device gain increases, the LVAD contributes a larger share of total aortic inflow and the fraction of beats with aortic-valve opening declines; in PV space this appears as a left-downward shift and a slimmer loop, consistent with stronger LV unloading. These trends recur for both HeartMate 3 and Corheart 6 within the tested range.

For the same aortic-flow target, CoHeart 6 settles at a substantially lower speed (2.8kRPM) than HeartMate 3 (4.68 kRPM). This implies a higher static hydraulic gain for CoHeart 6 (more flow per unit rpm at comparable head), *i.e.*, less rpm is needed to deliver the same perfusion.

HeartMate 3 shows a smaller first-peak flow overshoot but a longer settling envelope with slow decay of the speed ripple from 6.2 kRPM to 4.7 kRPM. Coheart 6 exhibits a larger initial overshoot yet settles faster toward 3.0 kRPM with minimal residual oscillation. Under identical PI gains and filtering, these contrasts are consistent with the pumps’ characteristic curves: higher plant gain (Coheart 6) → faster closed-loop and lower steady-state speed; lower gain (HeartMate 3) → slower decay and higher command.

In both cases the beat-wise average aortic flow converges to 5.4 L/min while the controller reallocates contributions between native aortic-valve ejection and LVAD flow through the speed command. The lower steady-state rpm of Coheart 6 suggests greater unloading per rpm (potentially lower shear for a given flow), whereas HeartMate 3 provides a slightly more tempered transient—useful trade-offs for pump selection and gain tuning.

4. Discussion

4.1. Methodological Advantages

1) Supervised variable focused on perfusion. Using total aortic inflow as the primary controlled variable directly constrains systemic perfusion. Compared with MAP-only or pump-head feedback, this target naturally captures pump-valve sharing and better reflects the clinical goal of delivering flow to the systemic circuit.

2) Robust measurement chain. Beat-to-beat averaging and taking the derivative on the mean attenuate intrabeat pulsatility and sensor noise, limiting differential amplification and reducing the risk of controller-induced oscillations.

3) Realistic actuator modeling. The controller explicitly uses the pump map

with instantaneous head ΔP , avoiding the oversimplification “fixed speed \approx fixed flow” and improving predictability across loading conditions.

4) Deployment simplicity. A positional PID with speed limiting and back-calculation anti-windup is lightweight, has few parameters, and is well suited to embedded real-time implementation.

5) Physiologic consistency. The 0D cardiovascular model includes AV delay and diode-valve logic; results reproduce expected LV unloading with left-downward PV-loop shifts and plausible changes in valve timing. These findings are consistent with prior research [11] [12], which has demonstrated similar PV-loop shifts as a hallmark of effective LV unloading, further supporting the physiological validity of the proposed control method.

6) Compared to other commonly used control targets in the literature, such as estimated left atrial pressure or pulsatility index, the mean aortic flow and pressure were selected as control targets in this study. These targets are more directly indicative of overall blood flow and heart unloading, making them well-suited to meet the dynamic physiological demands of different patients.

4.2. Existing Problems and Solutions

4.2.1. Existing Problems

The framework has practical and modeling constraints. First, performance depends on empirical pump maps, which can drift with viscosity, temperature, inter-patient variance, and device wear, biasing local gain and head estimates. Second, total aortic inflow is not routinely measurable; deploying this target will likely require additional sensors or a virtual-sensor strategy based on pressure and electrical variables, with added complexity and error sources. Third, the 0D model omits vascular inertance and valve opening dynamics and treats peripheral R/C as beat-wise constants, limiting representation of fast transients and reflex control. Fourth, beat-mean filtering introduces perceptual delay, potentially slowing response to acute load changes (posture, hemorrhage, vasoactive drugs). Fifth, no explicit suction detector is implemented; current safety relies on speed limits and averaging, leaving risk windows under extreme unloading. Finally, pathophysiologic heterogeneity (severe pulmonary hypertension, significant TR, arrhythmias) and real-time implementation issues (sampling, transport delays, quantization, packet loss) can degrade closed-loop quality and complicate patient-specific tuning.

4.2.2. Solutions

1) Online identification & gain scheduling. Use recursive estimation/Kalman filtering to track effective static gain and head sensitivity and schedule by operating region; perform slow pump-map self-calibration with projection/limits and fall back to a conservative parameter set when uncertainty grows.

2) Virtual sensing & sensor fusion. Combine motor current/torque with head estimates and aortic-pressure/valve priors in EKF/UKF to reconstruct total inflow; if differential-pressure or ultrasound flow is available, fuse signals with con-

confidence weighting and failure handling.

3) Minimal-state model refinement. Add key R-L-C inertance and simple orifice-valve dynamics in critical branches while constraining state growth to preserve real-time execution; pair with bounded estimators and noise shaping to capture fast transients without over-fitting.

4) Suction protection. Introduce explicit LV collapse indices (e.g., dP/dt patterns, suction proxies), a fault-management state machine with safe degradation, and hard constraints on speed, MAP, and pulse pressure.

4.3. Application Prospects

The system has broad clinical applications, both for initial device setup and for continuous autonomous adjustment. It can assist clinicians in setting the initial LVAD pump speed according to the patient's individual needs. Moreover, during long-term support, the system could autonomously adjust the pump speed in response to physiological changes, reducing the need for constant human intervention and improving the overall efficiency and effectiveness of patient care.

5. Conclusion

This work shows that an implementation-friendly PID speed controller—built on beat-mean measurements, derivative on the mean, and speed limiting (2 - 9 kRPM) with anti-windup—delivers physiologically consistent left-ventricular unloading with well-damped beat-scale dynamics under both flow-targeted and pressure-targeted modes. For flow targets (5.4/6.0 L·min⁻¹), the controller tracks from rest with a single modest overshoot (peak \approx 7.5 - 8.0 L·min⁻¹ within 10 - 20 beats) and short settling; steady speeds are \approx 4.68/5.68 kRPM on HeartMate 3 versus 2.80/3.18 kRPM on Corheart 6. For pressure targets (MAP = 85/95 mmHg), both devices again show lightly under-damped, exponentially convergent responses, requiring \approx 5.88/6.68 kRPM (HeartMate 3) versus 3.28/3.73 kRPM (Corheart 6), confirming that cross-device differences are dominated by pump-map gain rather than closed-loop damping. Across tests the transient envelopes (rise, single peak, settling within a few beats) are similar when gains are held constant, while the steady operating point needed to meet identical perfusion/pressure targets differs. PV-loop analyses consistently show left-downward shifts and slimmer loops at higher targets or higher effective gain, indicating stronger unloading with no suction observed in the tested window. Methodologically, supervising total aortic inflow/beat-mean variables ties control directly to systemic perfusion and naturally captures pump-valve sharing; together with anti-windup, this explains the observed beat-scale “second-order + integral” behavior and robustness. Clinically, the architecture supports a perfusion-first, pressure-safe hierarchical control (inner flow, outer MAP/pulse-pressure guards) and patient-specific tuning (valve-opening fraction, PV morphology), outlining a clear path to reliable, tunable LVAD speed control for both HeartMate 3 and Corheart 6.

Funding

This work was supported by National Natural Science Foundation of China (No. 52175263).

Conflicts of Interest

The authors declare no conflicts of interest regarding the publication of this paper.

References

- [1] Shahim, B., Kapelios, C.J., Savarese, G. and Lund, L.H. (2023) Global Public Health Burden of Heart Failure: An Updated Review. *Cardiac Failure Review*, **9**, e11. <https://doi.org/10.15420/cfr.2023.05>
- [2] Mancini, D. and Colombo, P.C. (2015) Left Ventricular Assist Devices: A Rapidly Evolving Alternative to Transplant. *Journal of the American College of Cardiology*, **65**, 2542-2555. <https://doi.org/10.1016/j.jacc.2015.04.039>
- [3] Mehra, M.R., Naka, Y., Uriel, N., Goldstein, D.J., Cleveland, J.C., Colombo, P.C., *et al.* (2017) A Fully Magnetically Levitated Circulatory Pump for Advanced Heart Failure. *New England Journal of Medicine*, **376**, 440-450. <https://doi.org/10.1056/nejmoa1610426>
- [4] Slaughter, M.S., *et al.* (2010) Clinical Management of Continuous-Flow Left Ventricular Assist Devices in Advanced Heart Failure. *The Journal of Heart and Lung Transplantation*, **29**, S1-S39.
- [5] Miller, L.W. and Rogers, J.G. (2018) Evolution of Left Ventricular Assist Device Therapy for Advanced Heart Failure: A Review. *JAMA Cardiology*, **3**, 650-658. <https://doi.org/10.1001/jamacardio.2018.0522>
- [6] Boston, J.R., Antaki, J.F. and Simaan, M.A. (2003) Hierarchical Control of Heart-Assist Devices. *IEEE Robotics & Automation Magazine*, **10**, 54-64. <https://doi.org/10.1109/mra.2003.1191711>
- [7] Arndt, A., Nüsser, P. and Lampe, B. (2010) Fully Autonomous Preload-Sensitive Control of Implantable Rotary Blood Pumps. *Artificial Organs*, **34**, 726-735. <https://doi.org/10.1111/j.1525-1594.2010.01092.x>
- [8] Liang, L., Meki, M., Wang, W., Sethu, P., El-Baz, A., Giridharan, G.A., *et al.* (2020) A Suction Index Based Control System for Rotary Blood Pumps. *Biomedical Signal Processing and Control*, **62**, Article ID: 102057. <https://doi.org/10.1016/j.bspc.2020.102057>
- [9] Castrodeza, J., Ortiz-Bautista, C. and Fernández-Avilés, F. (2022) Continuous-Flow Left Ventricular Assist Device: Current Knowledge, Complications, and Future Directions. *Cardiology Journal*, **29**, 293-304. <https://doi.org/10.5603/cj.a2021.0172>
- [10] Shavik, S.M., Zhong, L., Zhao, X. and Lee, L.C. (2019) *In-Silico* Assessment of the Effects of Right Ventricular Assist Device on Pulmonary Arterial Hypertension Using an Image Based Biventricular Modeling Framework. *Mechanics Research Communications*, **97**, 101-111. <https://doi.org/10.1016/j.mechrescom.2019.04.008>
- [11] Rubinstein, G., Lotan, D., Moeller, C., Slomovich, S., Oren, D., Fried, J., *et al.* (2023) (1060) The Hemodynamic Effects of Pump Speed Adjustments in Patients with Heartmate 3 Left Ventricular Assist Device. *The Journal of Heart and Lung Transplantation*, **42**, S458. <https://doi.org/10.1016/j.healun.2023.02.1271>

- [12] Qiu, Z., Song, X., Li, L., Shi, H., Xiao, L., Wu, Y., Rong, X., Fan, J., Wei, L. and Chen, X. (2025). Short- to Medium-Term Safety and Efficacy of the Implantable Corheart 6 Left Ventricular Assist System in Patients with End-Stage Heart Failure. *Chinese Journal of Clinical Thoracic and Cardiovascular Surgery*, **32**, 639-645.